IAC-05-D4.3.10

TESTING OF A TETHER DEPLOYMENT SYSTEM USING A COLD GAS THRUSTER

Steven van de Heijning (BSc)
Delft University of Technology, Netherlands
Stevenvandeheijning@hotmail.com

Ir. Barry Zandbergen (MSc)
Delft University of Technology, Netherlands
B.T.C.Zandbergen@lr.tudelft.nl

ABSTRACT

This paper describes the test of a tether deployment system using a cold gas thruster in a microgravity environment. The deployment system consists of a Hold Down and Release System (HDRS) and a tether end-body, which houses the cold gas thruster. The end-body connects to the tip of the tether, initially stored on a reel in a canister. The HRDS fixes the end-body to the canister prior to deployment and releases it after activation. An experiment rack fixes all the systems to the aircraft and ensures a deployment path free of obstructions.
The goal of the experiment is to determine a deployment profile, which sets out deployment time against deployed tether length, and to determine the behavior of the end-body and tether. The deployment velocity is determined from the measured rotational velocity of the reel. The motion of the tether and tether end-body is recorded using cameras.
The results show the possibility of using a cold gas thruster to start the deployment of the tether. The results though are heavily biased by the instability of the end-body and the residual acceleration of the aircraft.

1. INTRODUCTION

At the Delft University of Technology (DUT) research is performed on Electro-Dynamic (ED) tethers for power provision and propulsion purposes. Since the early nineties, several studies concerning the use of space tethers have been performed under the guidance of Ir. Zandbergen (MSc) and Prof. Ockels [1 – 5]. Currently an ED tether experiment is under development for Delfi-1, a micro-satellite with the purpose of enhancing space research and education at the DUT [6]. One of the objectives of the ED tether experiment is to demonstrate a successful tether deployment.

An ED tether is a simple idea, but one with an amazing number of uses. It is made up of two masses in orbit connected by a long, flexible, electrically conductive tape. Such an ED tether takes advantage of two basic principles of electromagnetism: current is produced when a conductive tape moves through a magnetic field, and the field exerts a force on the charged particles that make up the current. This principle can be used in three ways:

- Generate electric current flow to provide electrical power,
- Provide propellantless de-boost capability for spacecraft operating in Low Earth Orbit (LEO),
- Provide an acceleration force by adding a power source to the ED tether circuit.

Current research at DUT focuses on the development of a deployment system of a tether. Several options have been studied out of which springs and cold gas thrusters have been selected as the most promising[7]. Springs are common use for deployment systems and have proven to be capable of deploying km-long tether at relatively low velocity. Higher deployment velocities might be attainable with cold gas thruster, but

little experience is available. To gain more knowledge, a breadboard model of a deployment system using cold gas thrusters has been designed. To verify the design the following test platforms have been envisaged:

- DUT Rocket Test Facility [8], to determine the thrust characteristics,
- Parabolic flight, to test the deployment in a micro-gravity environment,
- Nano-satellite, like Delfi-C3[9], to test the tether deployment in a space environment.

This year, the test with the breadboard model was selected for flight on the ESA Student Parabolic Flight Campaign and a team of 4 students was put together. The experiment goals are to determine:

- A deployment profile, which sets out the deployment time against the deployed tether length, for the first meters of the deployment,
- The influence of the thrust plume and the shape memory effect on the tether during the deployment,
- The influence of the design of the propulsion system on the deployment.

For the development of the experiment, use was made of the experience gained in the previous parabolic flight campaign[10].

2. EXPERIMENT SETUP

The experiment consists of a canister, an end-body, instrumentation, an electrical system and a gas supply/storage system (figure 1). The canister holds the reel, onto which the tether is stored prior to deployment. The tether is fixed on one end to the reel and on the other to the end-body. The latter houses the cold gas thruster and the propellant tank. A Hold Down & Release System (HDRS) holds the end-body to the deployment canister prior to deployment and releases it after activation. Instrumentation includes a vane sensor, a pressure sensor and cameras. The vane sensor allows for the measurement of the rotational velocity of the reel, in order to determine the deployment velocity. The pressure sensor measures the pressure inside the tank on the end-body. The

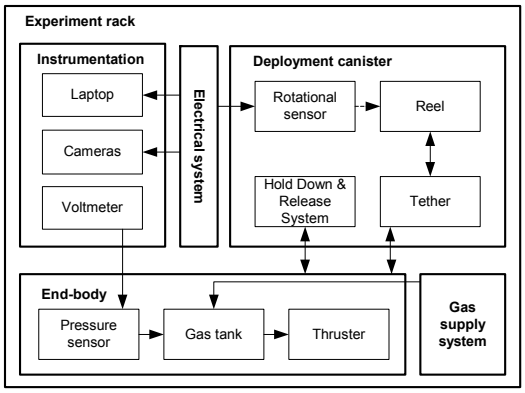

Fig. 1: Overview of the experiment systems and their interfaces

cameras are to record the motion of the tether and the end-body. A laptop and a voltmeter complete the setup and are to allow reading and storing the measurement data. A gas supply system allows for the filling of the propellant tank prior to each deployment. An experiment rack allows for mounting all the equipment, fixes the hardware to the aircraft and defines the deployment area.

The deployment is initiated manually and starts when the end-body is released, thereby automatically activating the thruster.

3. EXPERIMENT HARDWARE

A low-cost and short-time approach was used for the design of the experiment. Pre-tests performed on the DUT laboratory aircraft helped to finalize the design of the experiment hardware and to practice test procedures. A detailed description of the final test hardware is given hereafter.

3.1 End-body

Two types of end-body design have been constructed, one with a cross-shaped tank (figure 2) and one with a cylindrical tank (figure 3), which differ from each other by tank volume and mass inertia. The cross-shaped end-body has a larger mass inertia, but a smaller tank volume. An electrically operated actuating valve is used to start/stop thruster operation, thereby starting the deployment. The gas flows into a small chamber after which it leaves the thruster through an outlet of 2 mm in

diameter. For reasons of safety and low cost, air is used as propellant.

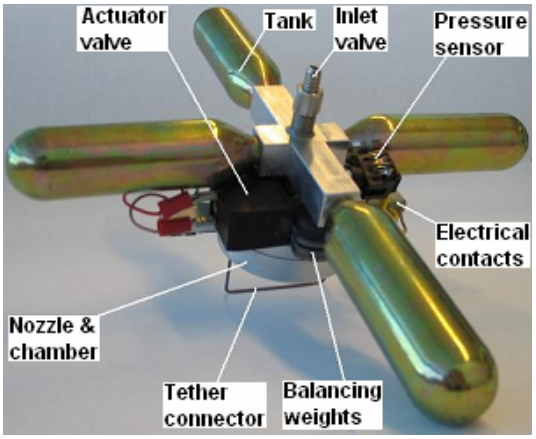

Fig. 2: Cross-shaped end-body

An ordinary bike tube valve is used as inlet valve, which allows refilling the tank after each deployment. The tether is connected to the end-body by wrapping it around the tether connector and fixing it with tape. The electrical contacts transfer the power to the actuator valve and the pressure sensor. They also transfer the pressure measurements to the voltmeter. Pieces of lead are used as balancing weights to align the center of mass with the thrust vector, see also section on 'balancing the end-body'.

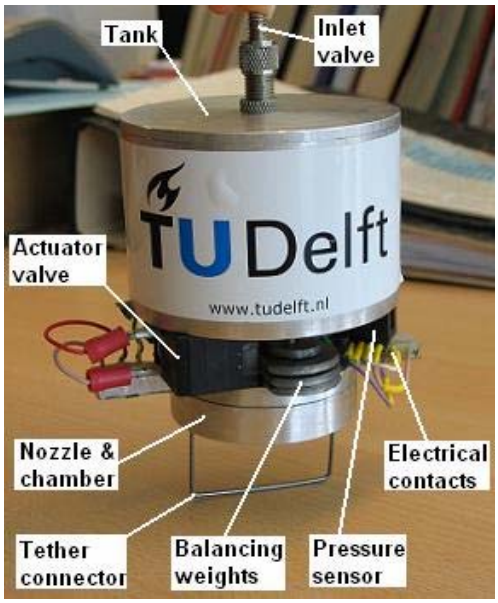

Fig. 3: Cylindrical end-body

3.2 Deployment canister

Figure 4 and 5 show the front and back of the deployment canister.

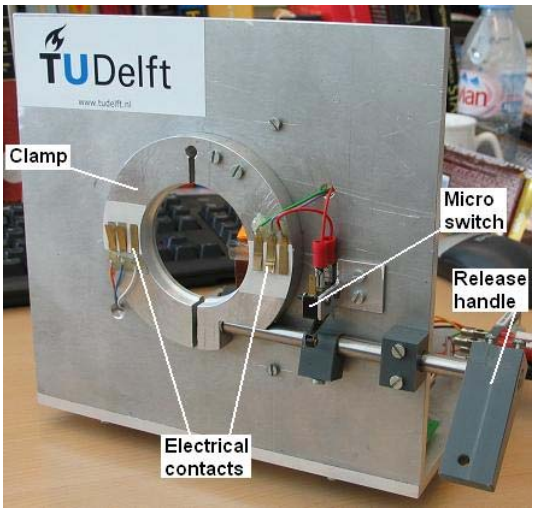

Fig. 4: Deployment canister front

The HDRS is on the front and connects the end-body to the deployment canister by placing the end-body chamber in the clamp, closing it with a screw. The electrical contacts make contact with the contacts on the end-body, thereby providing power to the actuator valve and pressure sensor.
With the release handle, the screw can be rotated thereby moving one arm of the clamp a fraction of a millimeter, which is enough to release the end-body. Just before release of the end-body, a micro-switch

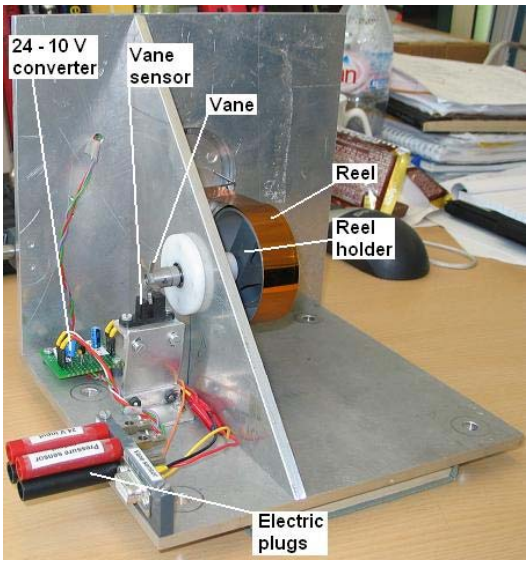

Fig. 5: Deployment canister back

turns off the power to the thruster actuator valve. The actuator valve opens and the thruster is activated.
Kapton-aluminium, 2 cm wide, 1,5 m long and 50 µm thick, is used as tether material and stored inside the canister on a reel. The reel is fixed to the axis by the reel holder and replaced after each deployment. Ball bearings are used to assure smooth rotation of the reel axis. A digital vane sensor measures the rotational velocity of the reel axis, which is used to determine the deployment velocity. The three electric plugs are needed to provide the experiment with power and to receive the data from the pressure and the vane sensor.

3.3 Experiment rack

The experiment rack consists of two base plates and a cage of 1 x 1 x 2 m, made out of aluminium profiles (figure 6). The deployment canister is positioned in the middle of the deployment area of 0,9 x 0,8 x 1,7 m. The base plates connect the cage and the experiment to the aircraft. The profiles are covered with padding for safety reasons. Nets are placed between the profiles to restrict the motion of the end-body. On one side the net can be slid away to provide easy access inside the cage. Lexan plates are put in front of the cameras to avoid impact with the end-body.

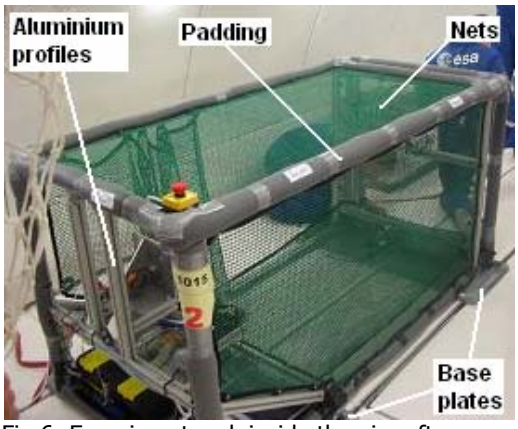

Fig 6: Experiment rack inside the aircraft

The front base plate is positioned below the deployment canister and secures the voltmeter, laptop, power converter and storage box. The storage box contains the 30 reels needed for each flight. The plate is covered with a Lexan plate to prevent impact with the end-body. The power converter provides power to the pressure sensor and the actuator valve.

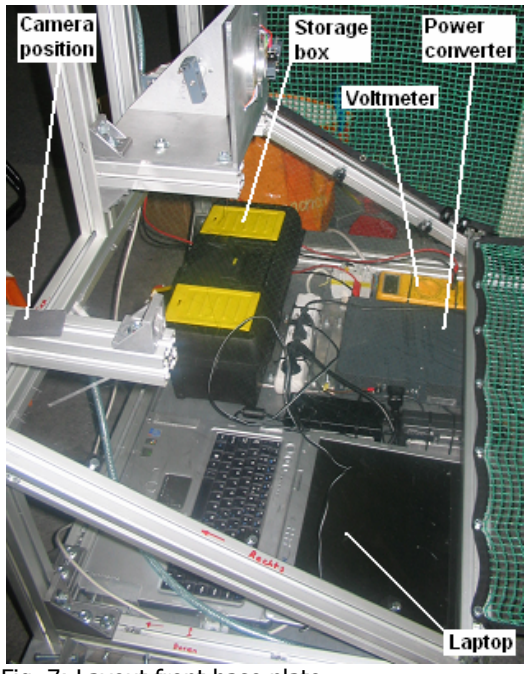

Fig. 7: Layout front base plate

The two cameras are connected to the aluminium profiles of the cage. One camera is positioned next to the deployment canister and perpendicular to the deployment direction (figure 7). The other camera is placed above the back base plate parallel to the deployment direction (figure 8). The back base plate fixes the gas storage tank of the gas supply system. Mounted on top of this tank is a regulator valve that limits the maximum fill pressure to 11 bar.


Fig. 8: Experiment rack backside

4. BALANCING THE END-BODY

Prior to flight the end-body is balanced, see figure 9. For this, small pieces of lead are used. The cross-shaped tank has 4 cylindrical tanks, which join in the middle, exactly above the nozzle. The balance weights are positioned in two places on the chamber, allowing balancing about both axes (horizontal plane). The cylindrical tank end-body is balanced using the cross-shaped tank, after which the tank is replaced by the cylindrical one.

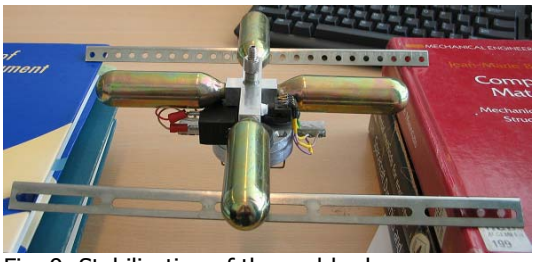

Fig. 9: Stabilization of the end-body

However, this does not ensure a well-balanced cylindrical end-body, because the pressure sensor is positioned on the tank somewhat to the side of the axis of symmetry of the tank. The balancing is performed with the naked eye, which also introduces some inaccuracy in the balancing of the end-bodies.

5. TEST RESULTS

This chapter first describes the in-flight acceleration levels. Second the results for the two types of end-bodies are given.

5.1 Flight accelerations

During the parabolas, flight acceleration levels have been measured relative to the aircraft fixed reference frame. The x_a-axis in this frame is in forward direction; z_a is from bottom to top (upwards) and y_a completes the right-hand orthogonal system. Typical results are shown in figure 10.

Results indicate that accelerations levels in the z_a-direction (vertical direction) are largest and of the order of several one-hundredths of a g. Accelerations in y_a- and x_a-direction are much more moderate and of the order of several one-thousandths of a g.

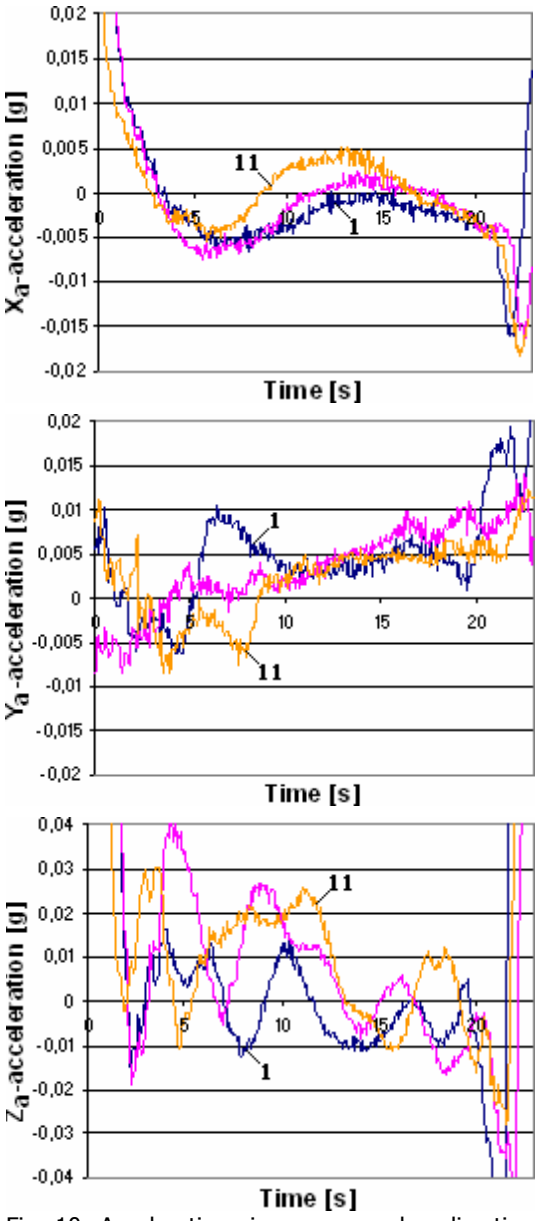

Fig. 10: Accelerations in x_a-, y_a- and z_a-direction for the 1st, 2nd and 11th parabola of the first flight.

5.2 Cylindrical end-body

During the first flight, 30 deployment tests were performed using the cylindrical end-body. The experiment fixed reference frame was defined such that y_e and z_e coincide with y_a and z_a. The x_e-axis was chosen opposite to x_a (positive to the back of the plane).

Due to an error in the pressure reduction valve of the gas supply system all

deployments were performed with an end-body tank pressure of maximum 7,5 bar in stead of the planned 11 bar. After the first 7 tests, the fill pressure in the tank could no longer be verified because the power connection of the pressure sensor broke down. To ensure that the maximum fill pressure was reached, extra time was taken to fill the end-body tank.

Deployment for all tests was activated after ± 7 seconds in the parabola to avoid the relatively large disturbances at the beginning of the parabola, see figure 10. During the first 3 parabolas, the tether got stuck behind the reel and reel axis and hence the end-body did not deploy successfully. As it was not possible to fix this problem during flight, it was decided to disconnect the tether and to use this opportunity to study the behavior of the end-body without tether affixed. However, even without tether affixed, several deployments failed because the end-body got stuck inside the HDRS.
During the majority of the remaining 'successful' deployments, it was found that the end-body moved in negative z_e-direction (down) and positive y_e-direction in the experiment fixed reference frame (figure 11).

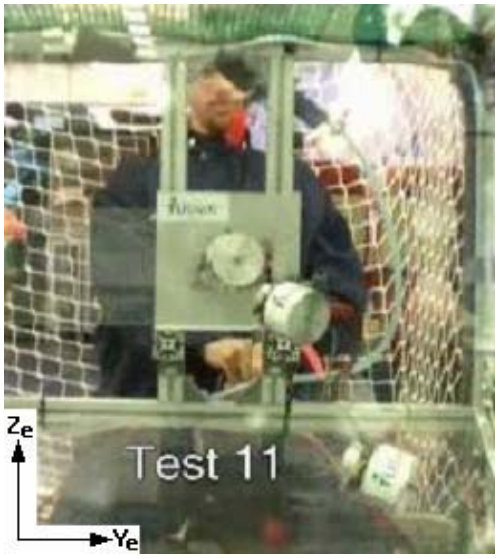

Fig. 11: Deployment of cylindrical end-body after 0, 1 and 2 seconds*

By disconnecting the tether, the deployment velocity in x_e-direction could not be determined from the vane sensor readings. It was also impossible to use the camera recordings to determine this velocity as the field of view of this camera turned out to be too limited. The motion of the end-body in y_e- and z_e-direction in the experiment-fixed frame was determined from the recorded images. The table 1 shows typical results for the motion in y_e-direction. The table also gives the rotation φ of the end-body around the x_e-axis.

Table 1: Motion of cylindrical end-body

#	Time†	Δφ	$\dot{\varphi}_{av}$	Δy_e	$v_{y,av}$
	[s]	[°]	[°/s]	[cm]	[cm/s]
1	2,9	60	21	16	6
4	3,2	130	41	27	9
5	3,0	40	13	3	1
9	2,9	95	33	20	7
11	2,6	90	35	25	10
12	2,8	100	36	20	7
13	2,7	75	27	14	5
16	2,7	50	18	3	1
18	3,3	140	43	28	9

During the tests, it was noticed that after the end-body hit the cage (the net), it slowly moved in negative x_e-direction (forward). This was attributed to the (average) acceleration of the plane in the parabola, which is in flight direction. The recordings of the in-flight acceleration as made by NoveSpace showed this in general to be true.
The recorded images revealed another unexpected phenomenon. Shortly after the end-body moved away from the deployment canister, it receives a little push in the deployment direction.

5.3 Cross-shaped end-body

21 (out of the planned 30) tests using the cross-shaped end-body were conducted during the 2nd flight. Difference in the test set-up as compared to the 1st flight, was that the entire cage was rotated 180 degrees so that the deployment was in the same direction as the (average) acceleration

* Videos of all the deployments can be found on www.protex2005.tk

† Time between activation and the moment the end-body is out of camera view

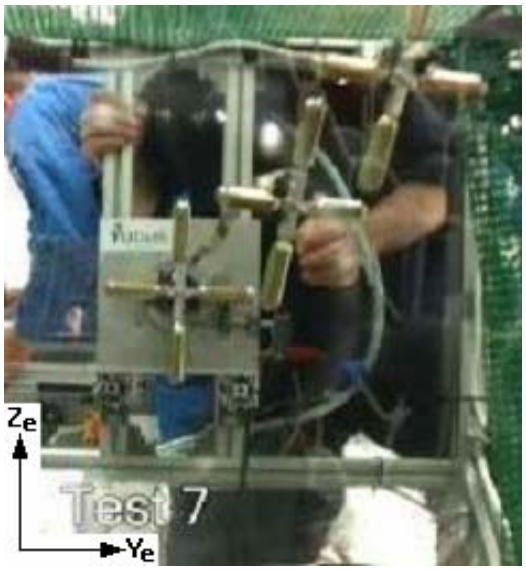

Fig. 12: Deployment of cross-shaped end-body after 0, 1,5 and 2,1 seconds

in aircraft direction Furthermore, the failed power connection of the pressure sensor was repaired after which it worked flawlessly. Also in contrast to the first flight, all experiments were made with the tether attached. It was expected that because of the 180 degree turn of the cage and the cross-shaped end-body, which is easier to balance, the end-body would not get stuck in the HDRS. This was confirmed by flight experiments until in test #21 the tether connector broke which made further testing impossible.

Of the 21 tests performed, 8 were invalidated, because the thruster actuator valve did not open on command. Of the remaining tests, several deployments were not recorded due to a malfunction of the front camera. A further problem experienced was that when initiating the thruster the exhaust jet blew the tether of the reel, creating a lot of slack tether. Although, this eliminated the measurements of the vane sensor, this did not lead to failure of the deployment.

In total 5 experiments were performed with useful recordings. The results of these experiments confirm that the end-body (mostly) moved in positive y_e- and z_e-direction (figure 12). The motion in x_e-, y_e- and z_e-direction, and the average total velocity with respect to the cage was determined from the recorded images. The results are given in table 2.

Table 2: Motion of cross-shaped end-body

#	Time† [s]	Δx_e [cm]	Δy_e [cm]	Δz_e [cm]	ΔL [cm]	v_{av} [cm/s]
3	3,7	64	18	20	70	19
4	2,4	35	5	16	39	16
5	2,1	26	6	16	31	15
7	2,5	76	22	23	83	33
8	1,9	26	2	16	30	16

6. ANALYSIS AND DISCUSSION

A remarkable result obtained during the test flights is the motion in y_e- and z_e-direction of the end-body. This is partly attributed to the thruster action and a rotation of the end-body as caused by the unbalance of the end-body. The faster the rotation, the further it moves in y_e-direction (figure 13).

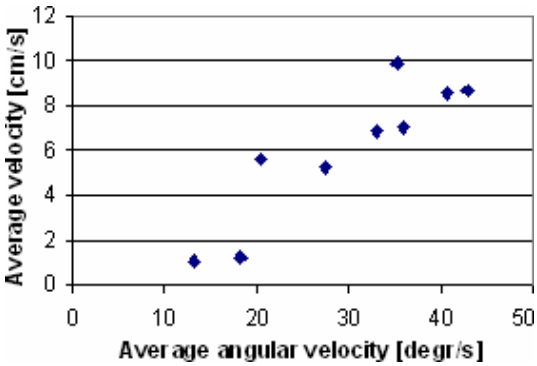

Fig. 13: Motion of the cylindrical end-body in y-direction

The cross-shaped end-body is easier to balance. Also the larger mass moment of inertia of this end-body compared to the cylindrical end-body leads to much smaller rotational accelerations, thus smaller rotations during the deployments. However, only 2 of the 5 deployments in table 2 did not show large rotations of the end-body.

Another reason is the residual accelerations of the aircraft. For instance, the 11th deployment in the first flight started around 8 s in the parabola, during which the accelerations in x_e, y_e and z_e are approximately -0,004g, 0,004g and 0,02g, respectively. The end-body is free-floating during the deployment and thus not subjected to these accelerations. Therefore, the accelerations of the end-body are

opposite with respect to the experiment cage. This means that the end-body 'moves' in positive x_e- and y_e-direction and in negative z_e-direction, see figure 11. That the end-body moves in positive y_e-direction is caused by the deflection of the thrust direction due to the rotation of the end-body. However, the acceleration in positive x_e is in contradiction with the in-flight observations, but comparing the aircraft accelerations of the 11th parabola with the 1st and 2nd parabola of the first flight, shows how irregular the aircraft acceleration levels for different parabolas are (figure 10). For example, the 1st parabola only creates accelerations opposite to the deployment direction.

The end-body being unbalanced and the residual accelerations also effect the deployment in the following ways:

- Directly after activation the end-body is stuck against the clamp of the HDRS.
- The end-body hits the clamp and rotates.
- The end-body hits the walls of the experiment rack before full deployment.

To prevent these effects, the deployment should be activated when the residual accelerations are the lowest. However, the irregularity of the acceleration patterns makes this impossible.

The small push forward shortly after activation of the deployment, as found in the first flight series, is possibly due to the thrust plume bouncing against the end-body after being reflected against the front of the deployment canister.
The development of slack tether immediately after thruster activation could also be a result of the thrust plume. The nozzle exit is placed exactly behind the tether connector allowing the thrust plume to get under the tether, still stored on the reel. The plume 'snatches' the tether from the reel, creating a tension force in the tether larger than the friction induced by the bearings and the magnetic field of the vane sensor. This induces a reel rotation in deployment direction, which rolls off the tether instead of being pulled off by the end-body.

From the recorded images, deployment profiles are determined. As an example, the profile of test 7 of the 2nd flight (test 2.7) is given (figure 14).

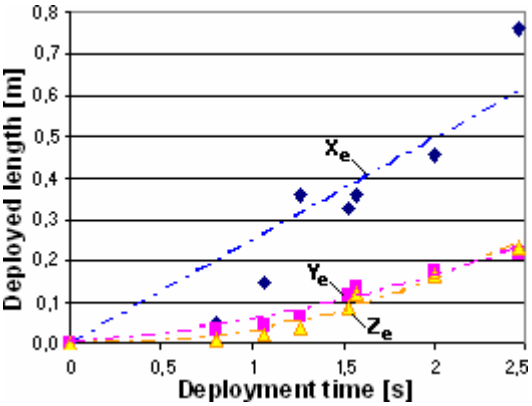

Fig. 14: Deployment profile test 2.7

According to theory, there is a linear relation between the deployed length in x_e-direction and the deployment time in the first few meters of the deployment[7]. The accelerations in y_e- and x_e-direction are assumed constant and therefore the dependency between deployment time and deployed length is approximated with a second order polynomial.
The end-body can only move 0,45 m to the sides and therefore test 2.7 lasted around 3,5 s. The motion in x_e-direction is governed by a combination of the thrust and the residual acceleration.

7. CONCLUSIONS & RECOMMENDATIONS

The experiment demonstrated the possibility of starting the tether deployment using cold gas thrusters. The cross-shaped end-body performed better than the cylindrical end-body. The deployment failures were mainly caused by a combination of unbalance in the end-body and residual acceleration of the aircraft.
Another important failure cause was that the thrust plume blew the tether from the reel directly after thruster activation.

To improve the experiment, it is recommended to:

- Improve the balancing of the end-body or by actively stabilizing the end-body for instance by using a gyroscope,

- Increase the thrust force by optimizing the design of the propulsion system,
- Determine the motion of the end-body more accurate by implementing a 3-axis accelerometer on the end-body,
- Enlarge the cage to obtain a longer deployment time,
- Avoid any interaction between thrust plume and tether.

ACKNOWLEDGMENT

The authors would like to express their thanks to the other members of the ProTEx team: Marcel Kwakkel, Emile Arens and Robin Raus for making this experiment a reality. Also thanks to:

- Bas Lansdorp for his advice and support during the project,
- Faculty of Aerospace Engineering, Chair of Control & Simulation, for providing the possibility to pre-test the experiment on the Cessna Citation II laboratory aircraft and special thanks to Kees van Woerkom, who gave us a lot of help and advice during the construction of the experiment,
- The people at the Instrumentation Workshop, who helped us during the design and construction of the experiment, in particular Bertus van der Stok,
- DUT and Faculty of Aerospace Engineering, Chair of Space Systems Engineering & Technology, for the funding of this project.

Fig. 15: ProTEx team

REFERENCES

1. Roozendaal, M.P.M., *Tethers in space, an overview*, Thesis rapport, Delft University of Technology, April 1988
2. Thoen, R.F.M., *Application of the gravity-gradient torque on a tethered system in a geostationary transfer orbit for the insertion of a satellite into the geostationary orbit*, Delft University of Technology, July 1999
3. Kruijff, M., Heide, E.J. van der, *StarTrack; a swinging tether assisted re-entry for the International Space Station*, EWP 1883, Delft University of Technology/ESA, 1996
4. Jainandunsing, S.A., *The combined electrodynamic tether and electric propulsion system*, Delft University of Technology/ESA, December 2001
5. Meeuwen, J. van, *Rockapult*, Delft University of Technology/ESA, 6 September 2002
6. Wijnans, A.S., Zandbergen, B.T.C., Kruijff, M., Heide, E.J. van der, *Bare electrodynamic tape tether experiment onboard the Delfi-1 university satellite*, 4th International Spacecraft Propulsion Conference, 2004
7. Heijning, S.P.A. van de, Zandbergen, B.T.C., *Design of an electro-dynamic tape tether deployment system*, IAC-05-C4.6.02, 56th International Astronautical Congress, 2005
8. Rycek, K.J.A., Bisi, L., Zandbergen, B.T.C., *Preliminary performance characterization of a 1N laboratory resistojet DUR-1*, IAC-05-C.4.4.01, 56th International Astronautical Congress, 2005
9. Ubbels, W.J., Hamann, R.J., et al, *Delfi-C3: a student nano-satellite as a test-bed for thin film solar cells and wireless onboard communication*, RAST, Turkey, 2005
10. Caluwaerts, D., Zandbergen, B.T.C, et al, *Deployment of an inflatable gravity gradient boom in micro-gravity*, IAC-05-A2.P.02, 56th International Astronautical Congress, 2005